Available online at www.sciencedirect.com
SCIENCE DIRECT®
Computers and Electronics in Agriculture 42 (2004) 31–42
Computers and electronics in agriculture
www.elsevier.com/locate/compag

Estimation of number and diameter of apple fruits in an orchard during the growing season by thermal imaging

D. Stajnko [a,*], M. Lakota [a], M. Hočevar [b]

[a] *Faculty of Agriculture, University of Maribor, Vrbanska 30, 2000 Maribor, Slovenia*
[b] *Faculty of Mechanical Engineering, University of Ljubljana, Aškerčeva 6, 1000 Ljubljana, Slovenia*

Received 18 June 2002; received in revised form 28 November 2002; accepted 13 May 2003

Abstract

A new method for estimating the number of apple fruits and measuring their diameter in the orchard was developed and tested. A thermal camera captured images of apple trees five times during the vegetation period June–September 2001. Each time 120 images of twenty apple trees were recorded late in the afternoon to achieve a temperature gradient between fruits and their background. Recorded images were processed using several image processing algorithms. Correlation coefficients R^2 from 0.83 to 0.88 were established between the manually measured fruit number and the estimated number based on a fruit detection algorithm. According to fruit development and the established growing curve, the value of the correlation coefficient, R^2, increased during the ripening period. For measuring the fruit's diameter values of R^2 between 0.68 and 0.70 were established. These slightly increased according to the fruit's colour and size development during the ripening period.
© 2003 Elsevier B.V. All rights reserved.

Keywords: Thermography; Image analysis; Apples; Yields; Diameters

1. Introduction

The question of future yield, its quality and economy of fruit-growing has always been the fundamental question for apple producers (Winter, 1986). Forecasting the number of fruit and size at harvesting represents together with ecological parameters, cultivar parameters

* Corresponding author. Tel.: +386-2-250-5800; fax: +386-2-229-6071.
E-mail address: denis.stajnko@uni.mb-si (D. Stajnko).

0168-1699/$ – see front matter © 2003 Elsevier B.V. All rights reserved.
doi:10.1016/S0168-1699(03)00086-3

and price parameters the basis for prediction of future yield, planning of incomes and calculation of profit (Welte, 1990). Since the 'Prognosfruit' Crop Forecast Model was developed and introduced in practice by Bavendorf Research Station (Winter, 1986), the yield has been estimated in many European countries using this procedure. The model is based on the yield capacity of the observed growing unit (trees, variety, rootstock, orchard age, slope, elevation and area), the fruit-set density of the growing unit in the given year and the average fruit mass at a harvesting date (Winter, 1986). However, as seen from the Prognosfruit annual report 2001, differences between the forecast and harvested yield have varied from −21.9 to + 14.1% per hectare in 2000 depending on the apple variety and country growing region (Lambrechts, 2001).

Currently, the 'Prognosfruit' Forecast Model is the only method accepted by the European apple and pear producers for yield quantity and quality estimation. The method predicts 97–98% of future yield for large growing areas with similar environmental conditions (for example 'Trento' in Italy or 'Lake Constance' in Germany) or for estimating average yield for whole countries (Lambrechts, 2001). However, the main disadvantage of the method is the time-consuming counting measurements of required parameters, which do not make it possible to predict the future yield in every individual orchard.

Potential enhancement of such forecasting methods can be achieved by applying visual techniques to collect of sample data. At present, in fruit growing, vision algorithms are used for detecting fruits by harvesting machines in experimental cases, but only under controlled lighting conditions (Jimenez et al., 1999).

With the first version of apple picking robot 'MAGALI', it was possible to detect different varieties of apple fruits when a protective coverage provided a dark background (Grand D'Esnon et al., 1987). As also reported by Juste and Sevilla (1991) the robot for harvesting oranges which was developed under the European Eureka Project required two flashlights for proper fruit detection. When testing three different strawberry harvesting robots Kondo et al. (1998) reported that there was a constant need for artificial light sources, although the ripe fruits were red in colour.

Similar artificial lighting requirements were reported by Tian et al. (1997) when sensing of different plants and discrimination of weeds from crop plants and soil was studied by using visual system under controlled illumination. However, using images formed with sunlight as an illumination source represents a greater challenge than using those created with controlled illumination. As noted by Steward and Tian (1998) direct sunlight causes substantial intensity differences within the images due to shadows and reflection from shiny leaf surfaces.

Effects of additional illumination on applicability of visual techniques was studied also by Peterson et al. (1999), who installed a fibre-reinforced drapery on an apple harvesting robot to block the influence of natural light conditions.

For determining the colour and shapes of weeds in cereal fields Perez et al. (2000) used a variant of the well-known Red/Green ratio measurement for predicting the number of seedlings and estimating the relative leaf area of crops and weeds, despite the difficulties with near ground images captured in natural lighting conditions.

Stajnko and Lakota (2001) found close correlation between the number of fruits obtained from image analysis and manually counted fruits, while detecting yellow and green–yellow 'Golden Delicious' fruit on the sunny side of apple trees under natural

lighting conditions. However, fruit detection on the images captured on the shaded side of the tree required artificially light source to sufficiently control illumination.

As opposed to these common visual techniques, thermography is based on sensing an object's own heat radiation. This enables evaluation of different characteristics of observed objects with the use of visual cameras. The authors have found few references concerning application of thermal imaging for determining plant parts, counting fruit, vegetable, seedlings or selecting weeds from plants and background. According to Lamprecht et al. (2002) a thermal camera showed promise for detecting temperature excess of certain thermogenic plants parts during anthesis. Three thermogenic plants, the foot yam *Amorphophallus paeniifolius*, the voodoo lily *Saurumatum guttatum* and the tropical water lily *Victoria cruciana*, exhibited a temperature increase of male flowers, appendices and floral chamber, up to 10 K.

In our research the number of fruits was also determined prior the harvesting period, when the colours of the fruits did not differ substantially from the colour of leaves. To overcome this problem thermal imaging, followed by image analysis techniques, was used instead of colour imaging. The objective on this paper is to demonstrate and evaluate the applicability of the method for predicting the number and the diameter of the apple fruits needed for calculating the current yield in an orchard.

The paper presents an algorithm able to threshold, count and report fruits' morphological characteristics from thermal images captured under natural conditions in the orchard. Then comparing predicted and actual numbers and diameters estimate the performance of the method.

2. Experimental methods

During the vegetative period June–September 2001 twenty apple trees were examined in the Faculty's four-year-old apple orchard. Apple trees were planted with the variety 'Golden Delicious' grafted onto M9 rootstock. Experiments were performed late in the afternoon, to ensure a temperature gradient between leaves and fruits due to their different heat radiation. The following developing stages of apple fruits were selected for capturing images in the crucial stages of the fruit's growth and development:

First stage—after fruit drop	June 6th 2001
Second stage—one month later	July 8th 2001
Third stage—one month later	August 16th 2001
Fourth stage—beginning of ripening	September 14th 2001
Fifth stage—collecting fruit	September 29th 2001

Three series of 20 pictures were captured on the sunny side of trees and another three series on the shadow side, both from the distance of 2.0 m at an angle of 90° to the planting row. Concurrently, on each photographed tree all fruits were manually counted and the diameter of ten sample fruits was measured with sliding calipers. Results were later compared with the thermal image analysis calculations.

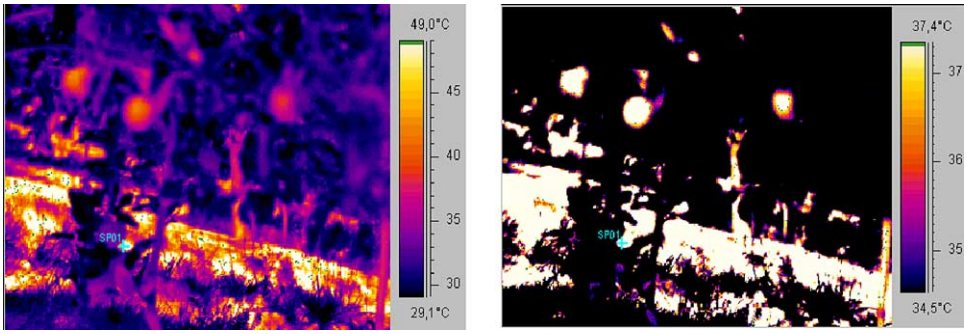

Fig. 1. Sample of thermal IMG image (320 × 240 pixels) before (left) and after temperature correction (right).

Thermal camera AGEMA 570 (Flir Systems^{TM}) was used for recording images. The emissivity of the object was set to 0.98. The resolution of the camera was 320 × 240 pixels and the temperature resolution was better than 0.5 °C.

2.1. Image format conversion

The AGEMA thermal camera supports its own IMG image format, which was converted into the better-known BMP format prior to further image processing. During this process, contrasts between fruits and background were extended by adjusting the temperature scale on each series of thermal images according to the average fruits temperature, as seen from Fig. 1.

2.2. Fruit detection algorithm

The discussion presented here will concern a whole set of images and is illustrated with the three images showing one sample tree (Fig. 2), chosen to be representative of the method's results. As seen from the first three RGB images ('a' column in Fig. 2), the thermal camera could not separate all fruits accurately. The RGB intensity, parts of soil, leaves and branches still appeared and interrupted the fruit detection, therefore the following steps were introduced in the algorithm.

The RGB intensity of fruits on the thermal images varied greatly according to the period of exposure to the sun-heat, so parts of apple fruits could not be detected. To overcome this problem, in the first step the data of a representative image from each series was transformed into a form which minimised the effect of RGB colour intensity variation on thresholding. The well known non-linear transformation from RGB components to the normalised chromaticity co-ordinates was employed, as follows:

$$r = \frac{R}{R+G+B}$$
$$g = \frac{G}{R+G+B} \quad (1)$$
$$b = \frac{B}{R+G+B}$$

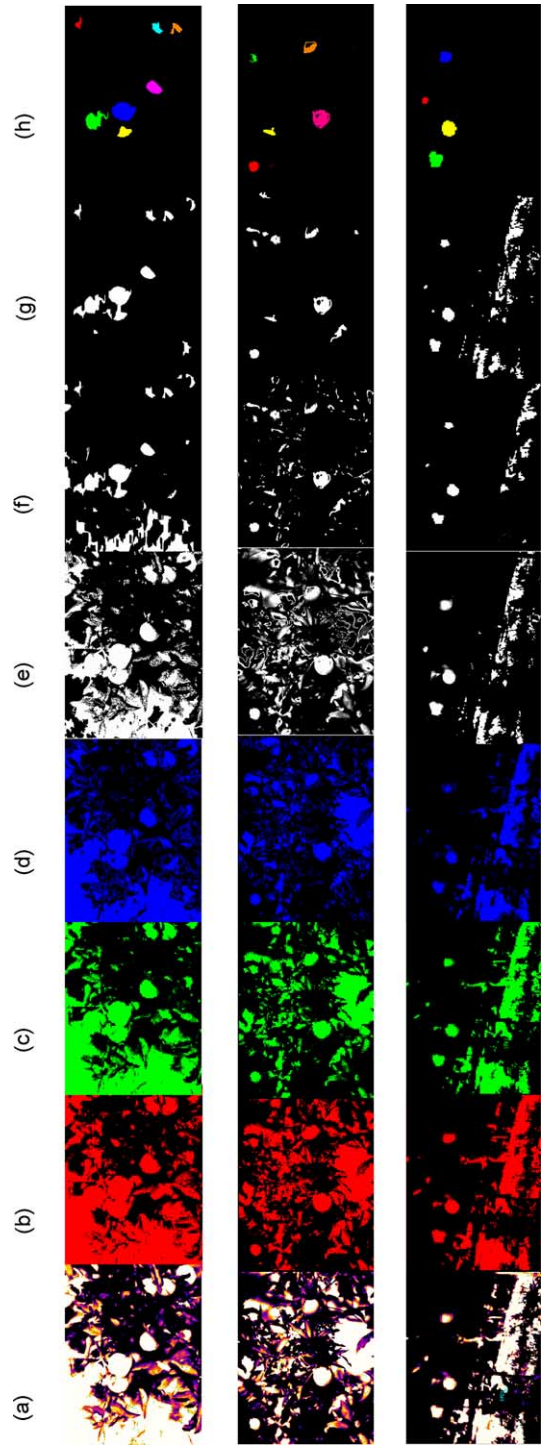

Fig. 2. Results of the algorithm. Column 'a': the RGB image after the IMG image conversion; column 'b': the Red image; column 'c': the Green image; column 'd': the Blue image; column 'e': the NDI image; column 'f': binary image (thresholded NDI image); column 'g': fruit and leaves separation; column 'h': result of the fruit detection.

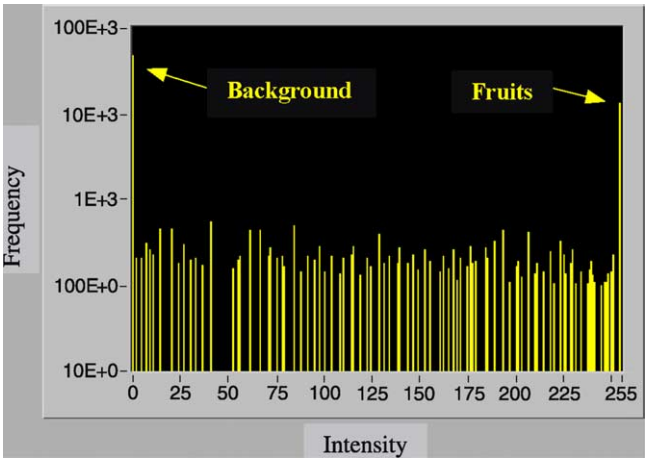

Fig. 3. Histogram (number of pixels) of the NDI image.

where r, g and b are the normalised values of the red, green and blue colour component of each pixel. Since $r+g+b=1$, this transformation maps all of the RGB colour space onto a plane which forms the edges of a colour triangle as it intersects the $R=0$, $G=0$ and $B=0$ planes.

As stated by Steward and Tian (1998) this transformation removes the intensity information from the data and reduces the dimension of the colour space, as the RGB space has a dimension of three, but the chromaticity co-ordinates have a dimension of two, because of the linearly by dependent relationship between equations.

However, by using such a simple method it was not possible to segment all pixels in the image accurately (columns 'b', 'c' and 'd' in Fig. 2), therefore a normalised difference index NDI using green and red images was additionally selected. Woebbecke et al. (1992) recommended the NDI as a very suitable method for distinguishing plants from the soil. This approach was defined as follows:

$$\mathrm{NDI} = \frac{g-r}{g+r} \tag{2}$$

The NDI index provides values between -1 and 1, because it is computed for all pixel values in the image. However for displaying the grey image, an interval from 0 to 255 was required, therefore 1 was added to all NDI index values and later multiplied by 128 to provide a 256 grey level interval. The NDI images are shown in the column 'e', Fig. 2 and a sample histogram is presented in Fig. 3.

The notable feature of the NDI image histogram is shown in the right peak corresponding to fruits and remaining noise pixels and in the left peak corresponding to background pixels.

Therefore a global threshold could be used to discriminate between background (soil, grass, sky) and parts of plants (leaves, fruits, branches). After nearly all leaves and fruits were separated from the background ('f' column in Fig. 2), using the NDI transformation and global threshold, in the following steps the fruit separation from leaves is shown ('g' in Fig. 2). Namely, the low contrast between fruits growing inside the crown and leaves

required additional filtering, so the image was developed through a morphological erosion which reduced the brightness of pixels that were surrounded by neighbours with a lower intensity. Then most of the misidentified pixels not connected to the fruit pixels did not appear in the final image. This operation was repeated until final segmentation between leaves and fruits was achieved. However, the original shape had to remain unchanged.

After the morphological erosion the image was filtered using a specified size of kernel (3×3 pixels) to remove the remaining noise. By applying the low-pass filter 'connectivity-4' two pixels were considered as part of the same object if they were horizontally or vertically adjacent.

Once pixels from leaves and fruits were established the differentiation between them had to proceed according to the selected template of apple fruit. The process included feature extraction, particle selection and classifier evaluation. Feature extraction included adjustment of horizontal and vertical resolution; particle selection matched each particle with the template mask, while classifier evaluation included major axis, length, width and longest segment measurements. The result of the processing is shown in column 'h', Fig. 2. Additionally, a file with detected fruits and characteristics was stored for later analysis. The data of the fruit longest segment was later used for calculating the diameter of the fruit according to the pixel/mm proportion.

Various commercial programs for performing the above described procedure exist. Among them, the IMAQ VISION 4.1.1. and LABVIEW 5.0.1. from National Instruments® were used in our research. Statistical analysis of results obtained manually and by thermal imaging were performed using SPSS Package Program.

3. Results and discussion

3.1. The number of fruits per tree

The number of apples per tree detected by the image analysis and manually counted is presented in Table 1. The fruit detection algorithm was tested for the number of apples between 8 and 120. Correlation coefficients R^2 from 0.83 to 0.88 were obtained for different developing stages of fruits and are shown in Table 1. Correlation curves for all the development stages are shown in Fig. 4a–e. The number of apple fruits slightly decreased from June to September. This decrease was due to apple fall caused by dry and hot weather in the summer. As seen, the value of correlation coefficient R^2 depended on the developing stage. The weakest correlation, $R^2 = 0.83$, was obtained at the first measurement on the June 6th, while the strongest $R^2 = 0.88$ correlation was achieved on the September 14th.

The reason for the increase of correlation coefficient during the fruits' ripening were the changes of their colour and diameter. Similar observations were reported from Kondo et al. (1998) for strawberry harvesting and Kataoka et al. (1999) for robotic apple harvesting.

However, these authors used visual imaging instead of thermal imaging. In their cases weaker correlation at the beginning of ripening was caused by lack of colour difference between leaves and fruits. With the thermal imaging method for fruit, due to their volume and colour, bigger and riper fruits can accumulate more heat than leaves and thus they radiate the heat later in the afternoon. So weaker correlation was detected at the beginning

Table 1
Number of apple fruits per tree measured manually and by thermal imaging at different developing stages

Number of apple fruits per tree										
Tree number	June 6th 2001		July 8th 2001		August 16th 2001		September 14th 2001		September 29th 2001	
	M	T	M	T	M	T	M	T	M	T
1	75	65	60	64	58	51	58	51	56	50
2	72	63	60	64	60	66	60	66	57	65
3	107	98	99	89	100	103	100	103	99	102
4	57	57	51	51	49	50	49	50	47	49
5	98	71	88	88	84	82	84	82	81	81
6	102	99	92	91	92	98	92	98	90	97
7	58	56	46	53	45	46	45	46	43	45
8	73	63	65	66	63	64	63	64	61	63
9	83	72	77	81	70	74	70	74	69	73
10	117	110	117	97	105	113	105	113	103	112
11	87	82	80	80	78	80	78	80	76	79
12	83	72	72	64	70	72	70	72	68	71
13	87	72	61	64	59	59	59	59	58	58
14	83	79	77	75	74	74	74	74	72	73
15	50	42	39	44	25	49	24	44	22	21
16	84	60	65	49	65	43	65	43	68	38
17	63	60	57	57	55	59	55	59	55	58
18	85	86	64	45	60	63	60	63	58	62
19	60	58	50	42	43	44	43	44	41	43
20	58	56	24	24	22	20	22	20	22	20
Average	79	72	66	64	64	64	64	64	62	63
R^2	0.83		0.83		0.87		0.88		0.88	

M, Manually; T, Thermal imaging.

of ripening when the difference in the heat capacity between leaves and fruits was not yet fully developed.

3.2. The apple fruit diameters per tree

The average predicted fruit diameters per tree for different developing stages of apple fruits are shown in Table 2. These averages were lower than the actual fruit diameters at all developing stages during the vegetative period. As seen in Table 2, the correlation coefficient R^2 varied slightly from 0.67 to 0.70, instead of the gradual increase observed in the correlation coefficients of the number of apples per tree. The reason for these lower coefficients is the underestimation of the apple fruit's diameter detected by the fruit detection algorithm based on the longest segment measurement. This algorithm is sufficiently accurate if a whole apple fruit is detected or a part of it is clearly seen. However, the edges of fruits have sometimes lower temperature or are hidden by leaves; thus lower fruit diameter is measured by thermal imaging and the weaker correlation coefficient is obtained.

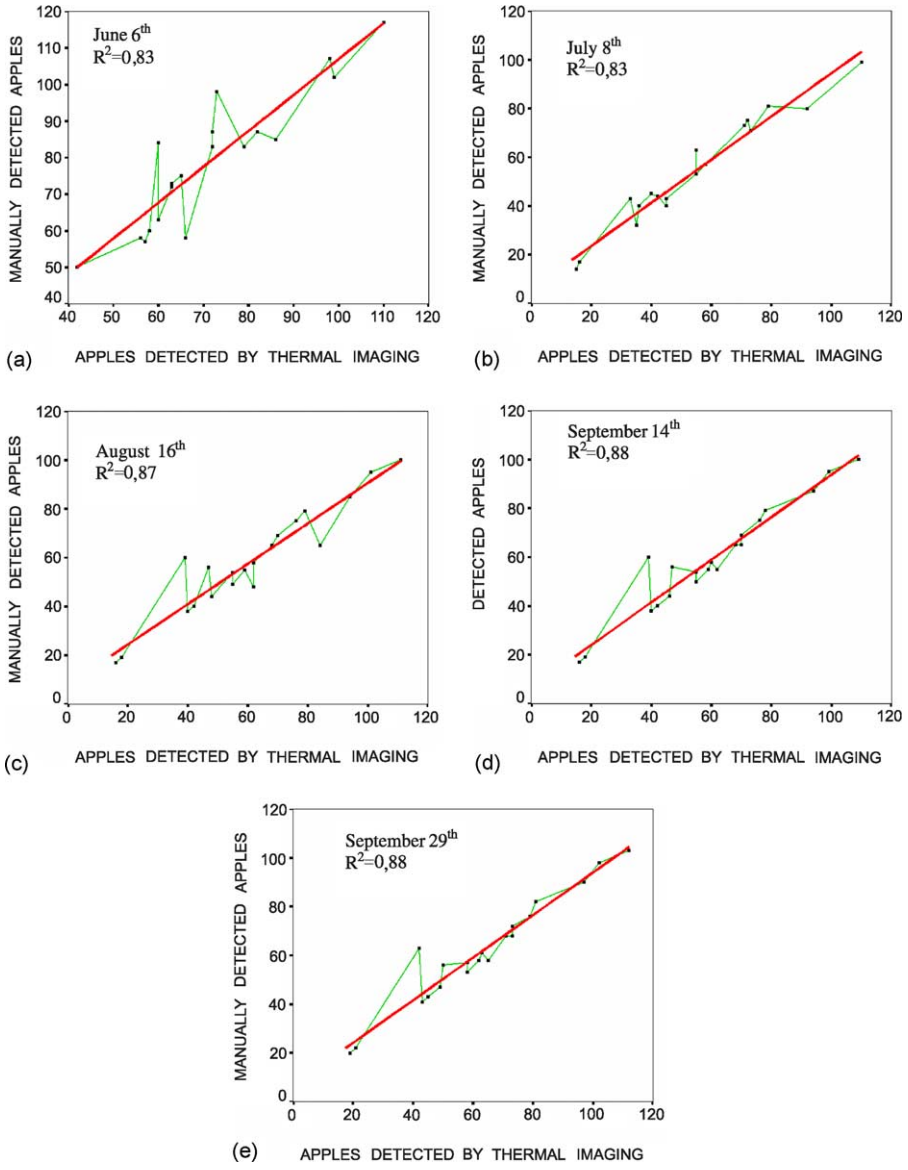

Fig. 4. (a–e) Correlation between manually counted and thermal image predictions of numbers of apples at different development stages.

Better results could be achieved, given a more advanced algorithm for calculating the apple diameter, including long term practical measurements from each variety.

Average apple fruit diameters at different development stages are shown in Fig. 5. It can be seen that the difference between manual measurement and thermal imaging decreased

Table 2
Correlation coefficients (R^2) for the average fruit's diameter per tree measured manually and by thermal imaging on the different developing stages

Date of sampling	Average fruit's diameter per tree in mm (manually)	Average fruit's diameter per tree in mm (thermal imaging)	R^2
June 6th	28	22	0.68
July 8th	39	34	0.69
August 16th	62	57	0.67
September 14th	69	66	0.69
September 29th gathering	69	67	0.70

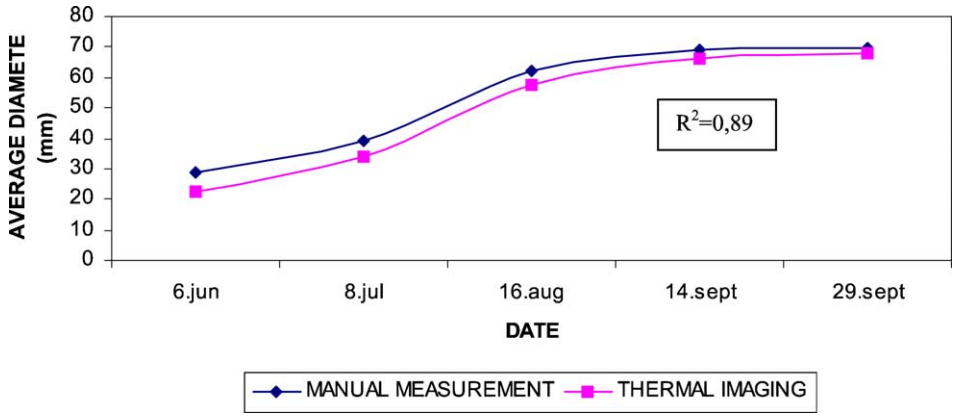

Fig. 5. Curve of the fruit's diameter development estimated by thermal imaging and by manual measurements.

during the vegetative period. It was largest at the fruit drop period in June and smallest at the harvesting period. When comparing the curve of manual measurements and calculated diameters from the thermal imaging, a strong correlation coefficient $R^2 = 0.89$ could be estimated. Furthermore, the curve of apple fruit development obtained in our research was very similar to the results estimated by Welte (1990) in his 10-years' observations.

3.3. Properties of fruit detection algorithm

The fruit detection algorithm is based on evaluating the temperature difference between fruits and the background. The major part of the heat is accumulated in the fruits directly from the sunshine and it is later radiated into the surroundings. Contrary to the fruits, leaves accumulate significantly less heat and radiate it for a shorter time. Furthermore, bigger and riper fruits can accumulate more heat than the smaller ones. For this reason, weaker correlation for the number of fruits per tree was detected in June and July than later in August and September.

However, the fruit position on the crown is another factor affecting the efficiency of the algorithm. By their position on the tree leaves prevent sunshine heating all fruits to the same degree for the same period. Fruits inside the crown are exposed to the sunshine for a shorter time than those outside the crown, so they could be cooled in almost the same period as

leaves. For that reason, the thermal camera could hardly detect the temperature gradient between inner fruits and leaves. However, none of the mentioned parameters reduce the accuracy of counting fruits, because the fruit is already detected by the algorithm, when just a part of it radiates gradient heat.

In contrast, the fruit position on the crown does effect the accuracy of diameter estimation. Fruit diameter would be underestimated if parts of fruits were covered by leaves or branches. In that case the measured fruits could appear not only circular, but also triangular, square or polygonal and therefore could induce fixed errors to the fruit detection algorithm. By introducing the longest segment algorithm the correlation coefficient R^2 was increased to the more promising 0.70. However, for more precise diameter estimation, refined algorithms including fruit development parameters and variety characteristics need to be added.

4. Conclusions

The proposed measuring technique based on thermal imaging and analysis can be employed to provide an objective and easy counting of apples and measurement of their diameters needed for calculating of apple yield. In comparing with the current method of manual sample counting, it enables faster investigation of larger sample orchard.

The system was used successfully during the whole vegetative period June–September in all cases when only a small part of the apple was detected. However, it was not always able to distinguish between fruits and leaves growing deep in the tree-crown. Further work is needed to study these particular cases by implementing a shape recognition procedure to the algorithm so that it is possible to detect a hidden spherical object by obtaining a set of pixels corresponding to its boundaries. When fully developed, a machine vision system could be employed for a real-time orchard operation.

Acknowledgements

This research was funded by The Ministry of Agriculture, Forestry and Food of the Republic of Slovenia. Project number No. V4-0199-98. The funding is gratefully acknowledged.

References

Grand D'Esnon, A., Rabatel, G., Pellenc, R., 1987. Magali: a self-propelled robot to pick apples, ASAE paper No. 87-1037, St. Joseph, MI 49085-9659.

Jimenez, A.R., Jain, A.K., Ceres, R., Pons, J.L., 1999. Automatic fruit recognition: a survey and new results using range/attenuation images. Pattern Recog. 32, 1719–1736.

Juste, F., Sevilla, F., 1991. Citrus: a European project to study the robotic harvesting of oranges, Proceedings of the Third International Symposium Fruit, Nut and Vegetable Harvesting Mechanization, Denmark, Sweden, Norway, pp. 331–338.

Kataoka, T., Bulanon, D.M, Hiroma, T., Ota, Y., 1999. Performance of robotic hand for apple harvesting, ASAE Paper No. 99-3003.

Kondo N., Hisaeda K., Monta M., 1998, Development of strawberry harvesting robotic hand, ASAE Paper No. 98-3117.

Lambrechts, G., 2001. Apple EU 2001, Forecast 2001, Prognosfruit 2001, pp. 1–8 http://cmlag.fgov.be/dg2/fr/Communications/prognos-algemeen.pdf.

Lamprecht, I., Schmolz, E., Blanco, L., Romero, C.M., 2002. Flower ovens: thermal investigation on heat producing plants. Thermocimica Acta 7051, 1–12.

Perez, A.J., Lopez, F., Benlloch, J.V., Christensen, S., 2000. Colour and shape analysis techniques for weed detection in cereal fields. Comput. Electron. Agric. 25, 197–212.

Peterson, D.L., Anger, W.C., Bennedsen, B.S., Wolford, S.D., 1999. A system approach to robotic bulk harvesting of apples. ASAE Paper No. 99-1075.

Stajnko, D., Lakota, M., 2001. Using image processing and analysis techniques for counting apple fruits in the orchard. Horticultural Sci. (Prague) 28 (3), 95–99.

Steward, B.L., Tian, L.F., 1998. Real-Time Machine Vision Weed-Sensing. ASAE Paper No. 98–3033.

Tian, L., Slaughter, D.C., Norris, R.F., 1997. Outdoor field machine vision identification of tomato seedlings for automated weed control. Trans. ASAE 40 (6), 1761–1768.

Welte, H.F., 1990. Forecasting harvest fruit size during the growing season. Acta Horticulturae 276, 275–282.

Winter, F., 1986. Modelling the biological and economic development of an apple orchard. Acta Horticulturae 160, 353–360.

Woebbecke, D.M., Meyer, G.E., Von Bargen, K., Mortensen, D., 1992. Plant species identification, size and enumeration using machine vision techniques on near-binary images. SPIE Optics Agric. Forestry 1836, 208–219.